ACS BIO & MED CHEM Au
AN OPEN ACCESS JOURNAL OF THE AMERICAN CHEMICAL SOCIETY

pubs.acs.org/biomedchemau

Article

Amphiphilic Membrane Environments Regulate Enzymatic Behaviors of *Salmonella* Outer Membrane Protease

Siau Ling Kum,[⊥] James C. S. Ho,[⊥] Atul N. Parikh, and Bo Liedberg*

Cite This: *ACS Bio Med Chem Au* 2022, 2, 73–83

Read Online

ACCESS | Metrics & More | Article Recommendations | Supporting Information

ABSTRACT: The role of an amphiphilic environment in the functional regulation of integral membrane proteins is well appreciated but how specific amphiphilic surrounding influences the conformational plasticity and function of a protein is less obvious. We focus on the *Salmonella* phosphoglycerate transport system (pgt)-encoded outer membrane protease E (PgtE), which plays an important role in tissue infiltration and survival of *Salmonella enterica*. Despite our understanding of its physiological functions, elucidation of its enzymatic behavior in response to the immediate amphiphilic surrounding is lacking. We monitor the proteolytic activity of PgtE reconstituted in Zwittergent 3-12 detergent micelles or a 1-palmitoyl-2-oleoyl-glycero-3-phosphocholine (POPC) bilayer and examine factors that influence its activity. We find, to our surprise, that PgtE, which is thought to elicit a rapid response toward various substrates, showed hysteretic enzymatic behavior, characterized by a prominent lag phase prior to achieving the exponential steady state in its detergent-stabilized form as well as in the outer membrane embedded native state in live bacteria. The lag phase was abolished under three conditions: preformation of an inactive detergent-stabilized PgtE−substrate complex without lipopolysaccharide (LPS), LPS-bound detergent-stabilized PgtE that had reached steady state velocity, or PgtE reconstituted into a POPC bilayer environment. Interestingly, detergent- and bilayer-stabilized PgtE showed comparable steady-state activity. And strikingly, lipopolysaccharide (LPS) becomes nonessential for the activation of PgtE when the protein is reconstituted in the phospholipid bilayer, contrasting a long-standing notion that LPS is required for proteases belonging to the omptin family to be proteolytically active. These findings suggest intriguing biological nuances for the proteolytic function of PgtE that were not well appreciated previously and offer new perspectives that may generally be applicable for omptins.

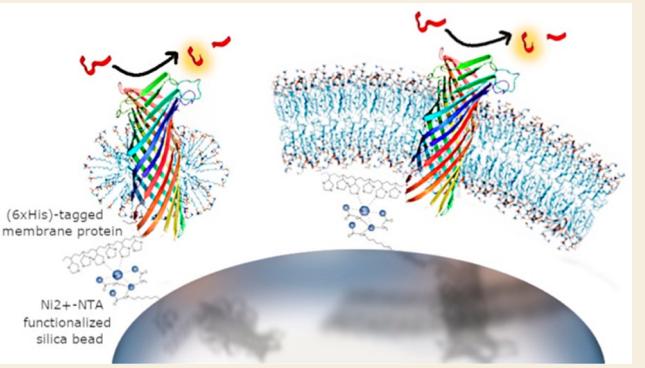

KEYWORDS: *PgtE, omptin, outer membrane protease, hysteretic enzyme, proteolytic activity, membrane protein reconstitution*

INTRODUCTION

Integral membrane proteins are closely dependent on their amphiphilic environment to ensure proper functional manifestation of conformational plasticity.[1,2] For the biogenesis of a distinct group of integral membrane proteins, the outer membrane proteins (OMPs) which are found almost exclusively on the outer membrane of Gram negative bacteria,[3,4] additional pathways are crucial. This involves, for example, multistep chaperone-assisted trafficking and folding[3,5,6] across the periplasmic space into a crowded, highly ordered, and asymmetric lipid bilayer.[7−10] To study the structure and function of membrane proteins, *in vitro* systems involving detergents,[11] liposomes,[12] nanodiscs,[13] or amphiphilic polymers[14,15] are used to stabilize the functional forms of membrane proteins outside their native environments. Despite advances in protein structure elucidation and their association with different functional states, our understanding of how the environments may influence the behaviors of membrane proteins[3,16] lacks predictive capability to faithfully reproduce the interplay between the protein and lipids.[17−22]

The omptin family of outer membrane proteases, most commonly represented by outer membrane protease T (OmpT) of *Escherichia coli*, plasminogen activator (Pla) of *Yersinia pestis*, and PgtE of *Salmonella enterica*, targets the host immune response components and elicits varying pathogenesis.[23] Out of the three proteases, OmpT and Pla are comparatively well understood molecularly, owing partly to the availability of their crystal structures, whereas PgtE is less studied. Our current understanding of PgtE arises from a wealth of literature on its physiological functions, which

Received: August 3, 2021
Revised: September 27, 2021
Accepted: October 27, 2021
Published: December 14, 2021

https://doi.org/10.1021/acsbiomedchemau.1c00027
ACS Bio Med Chem Au 2022, 2, 73–83

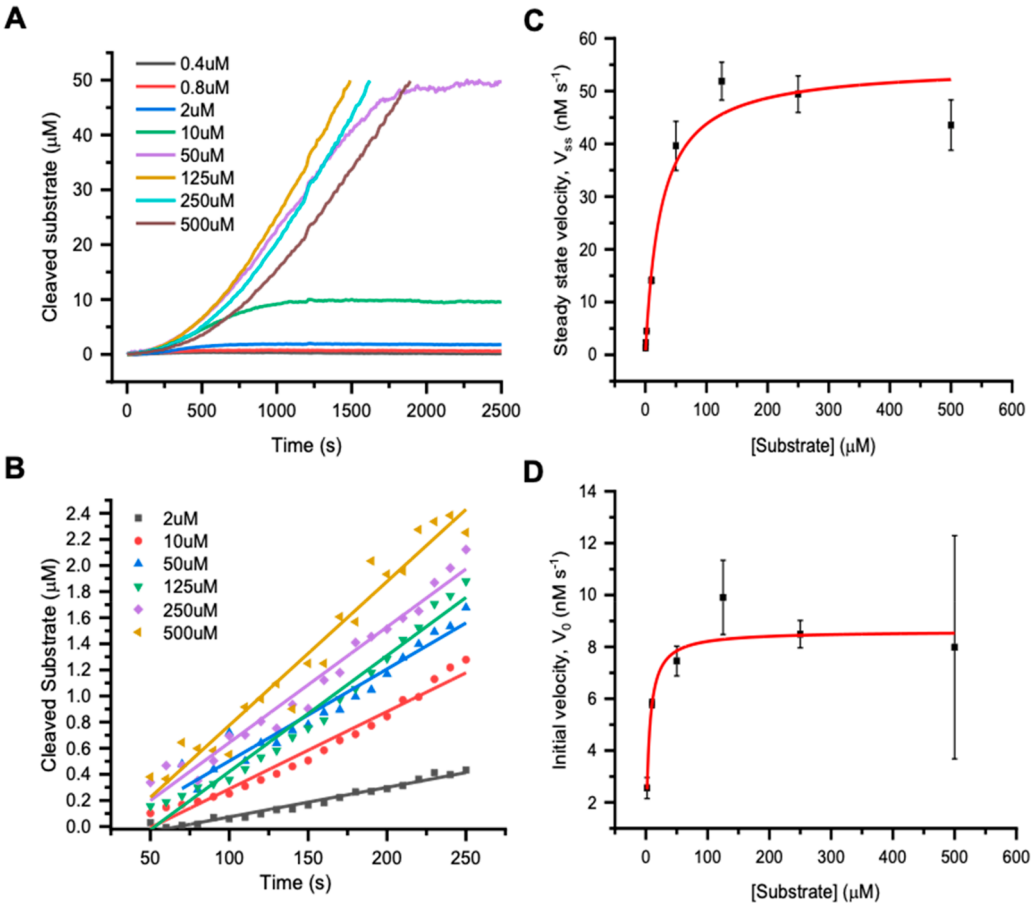

Figure 1. Enzyme kinetics of Zw12-PgtE. (A,B) Representative progress curves of Zw12-PgtE as a function of substrate concentration. The full progress curves (A) and the first 250 s of the same plot (B) are shown. The progress curves for 125, 250, and 500 μM are truncated at Y = 50 mM cleaved substrate, as the fluorescence intensity does not increase linearly above 50 μM. (C,D) Michaelis−Menten plots of the enzymatic activity of Zw12-PgtE against the substrate concentration. The steady-state velocity V_{ss} (C) and initial velocity V_0 (D) are calculated. Error bars indicate the standard deviation for two independent measurements. Michaelis−Menten plots were used to calculate kinetic parameters: V_{max} and k_{cat}.

include its effects on plasmin regulation,[24−28] the complement components,[29,30] the coagulation pathway,[25,27,28] the matrix metalloproteinase system,[31] and antimicrobial peptides.[32] The combined effect is an enhanced tissue infiltration and expansion of the bacteria.[23] Complementing the presence of a largely impermeable outer membrane, this set of structural and functional attributes enables successful colonization of the host. A molecular understanding of how PgtE functions as an enzyme within its immediate surrounding environment[33] has not been well resolved.

A unique requirement for the proteolytic function of omptins is the binding to lipopolysaccharide (LPS) as a cofactor.[24,34,35] It has been proposed that LPS binding to a putative binding site triggers a subtle structural change, which results in proteolytic activity, largely based on the OmpT structure.[34] Furthermore, the interaction with LPS has been linked to a protective role in the autoproteolysis of OmpT.[36] The mechanisms are poorly understood,[35] however, and this view has been debated with a recent report showing that the putative binding site is not essential for the binding of LPS and that LPS does not protect folded OmpT from self-cleavage.[37] This discrepancy in fundamental structure−function understanding of omptins highlights the considerable challenge in reproducing the function of the biogenesis pathway[6] outside of the native environment,[10] and more work is needed to resolve the underlying molecular details.

We studied the enzymatic behavior of PgtE in free-floating micelles and bead-immobilized micelles or a phospholipid bilayer and aimed to gain a deeper understanding of its enzyme behavior within these amphiphilic scaffolds. We find, to our surprise, that PgtE, thought to function efficiently in its protective response toward the instantaneous rise in the concentration of substrates, exhibits hysteretic enzymatic behavior in its purified detergent-stabilized form as well as in the outer membrane embedded native state in live bacteria. This behavior is influenced by its solubilizing environment and substrate availability. Additionally, we find that LPS becomes nonessential for the activation of PgtE when the protein is reconstituted in a phospholipid bilayer, thus contrasting a long-standing notion that LPS is required for omptins to be proteolytically active.[34] The environment-sensitive hysteretic enzymatic behavior of PgtE, along with the altered role of LPS, suggests potentially important and underexplored biological nuances, at least within the omptin family of proteases.

RESULTS AND DISCUSSION

Production of Recombinant PgtE and Protease Assay Optimization

Recombinant hexahistidine tagged PgtE was overexpressed as inclusion bodies and solubilized in 8 M urea prior to detergent-assisted refolding using Zwittergent 3-12 (Zw12, 31 mM) to

https://doi.org/10.1021/acsbiomedchemau.1c00027
ACS Bio Med Chem Au 2022, 2, 73−83

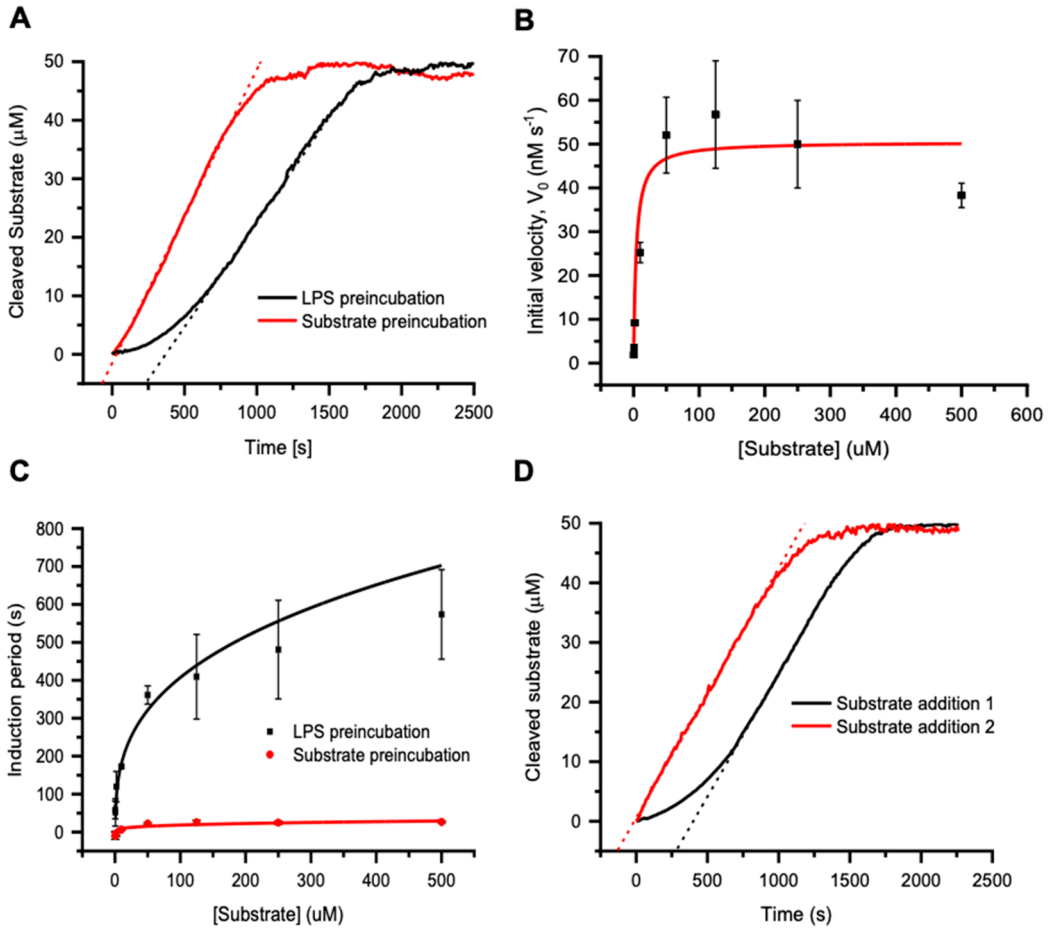

Figure 2. Effect of preconditioning on the enzymatic behavior of Zw12-PgtE. (A) Representative progress curves of Zw12-PgtE with a 15 min LPS preincubation or a 10 min substrate (synthetic peptide substrate Abz-ARRA-Tyr(NO_2)-NH_2) preincubation. (B) Michaelis−Menten plot of the enzymatic activity of Zw12-PgtE after being preconditioned with the substrate. Error bars indicate the standard deviation for two independent measurements. (C) Induction period of Zw12-PgtE activity with two different preconditioned steps as a function of substrate concentration. Error bars indicate the standard deviation for two independent measurements. (D) Progress curves of Zw12-PgtE with the first substrate addition after LPS preincubation (substrate addition 1) and addition of new substrate (substrate addition 2) upon enzyme activity ceased due to the natural depletion of substrate addition 1. The measurement time points for the two sequential measurements are overlaid for visual comparison.

obtain detergent-stabilized PgtE (Zw12-PgtE), following a similar strategy used for OmpT.[37,38] LC-MS analysis of the PgtE sample displayed three peaks (32671.59, 65312.50 and 65261.29), which matched the theoretical molecular weight of PgtE with molecular ion adducts (Figure S1A), thus confirming the identity of the overexpressed PgtE. SDS-PAGE of PgtE after 10 min of heating at 100 °C showed two major protein bands at ∼32 and ∼27 kDa as well as a faint ∼13 kDa band (Figure S1B). Subjecting excised bands from the gel for MALDI-TOF mass spectrometry analysis, we confirmed the identity of the two higher molecular weight bands to be PgtE (protein score of 222 and 158, respectively). The third band did not produce a hit, indicating a trace amount of impurities. Furthermore, the intensity of the lower molecular weight band at ∼27 kDa relative to total intensity of the two bands was reduced from 10% to 2% upon extended heating at 100 °C for 45 min (Figure S1C), consistent with the heat modifiable property of homologous proteins.[37,38] Based on gel densitometry analysis, the purity of the PgtE was ∼95%.

A set of variables including LPS:enzyme stoichiometry, assay pH, and buffer composition were systematically tested using a FRET-based activity assay,[37,38] and maximum steady-state velocity ($V_{max,ss}$) for each condition was determined to identify the optimal assay condition for Zw12-PgtE. (Note: Determination of the enzyme kinetic parameters including $V_{max,ss}$ is described in the subsequent section.) Our starting buffer condition was 2 mM Zw-12, 20 mM Bis-Tris, 5 mM EDTA, pH 6.2, similar to that reported for OmpT.[37] By varying Zw12-PgtE and LPS concentrations, the $V_{max,ss}$ of Zw12-PgtE increased with an increasing amount of enzymes and saturated at approximately equimolar concentration of LPS for each Zw12-PgtE concentration tested, suggesting 1:1 LPS/Zw12-PgtE binding (Figure S2). With a vanishing amount of LPS, V_{ss} approached zero, consistent with the notion that LPS is required for the protease activity.[24,34,35] Next, a range of pH from 5.0 to 8.0 was examined and an optimal working pH range from 5.0 to 6.2 was identified (Figure S3A,B). A further increase in assay pH (6.7 to 8.0) abolished the Zw12-PgtE activity completely. Thus, subsequent experiments were performed with an equimolar LPS:enzyme stoichiometry at pH 6.

Next, we tested different assay buffer compositions to further optimize the assay. Zw12-PgtE was found to be most active in the assay buffers containing 20 mM Bis-Tris, 5 mM EDTA, with or without 2 mM Zw12 detergent (Figure S3C). As Zw12-PgtE was refolded in 31 mM Zw12 detergent, a working

https://doi.org/10.1021/acsbiomedchemau.1c00027
ACS Bio Med Chem Au 2022, 2, 73−83

concentration of 4.5 mM Zw12, which is above the critical micellar concentration of Zw12 (CMC = 2−4 mM), was achieved after dilution of the stock Zw12-PgtE in the assay volume. Furthermore, the inclusion of EDTA and the use of Bis-Tris (as compared to PBS) were found to be important for activity.

The optimal assay condition selected for Zw12-PgtE consisted of 20 mM Bis-Tris, 5 mM EDTA, 2 mM Zw12 at pH 6, along with LPS at equimolar LPS:enzyme stoichiometry.

Enzyme Behavior of Zw12-PgtE

We examined the activity of Zw12-PgtE as a function of substrate concentration using the identified assay condition. The increase in fluorescence intensity (corresponding to accumulation of cleaved substrate, Abz-ARRA-Tyr(NO_2)-NH_2) within the first 250 s was substantially slower than that of the exponential phase within the next 1000 s for all substrate concentrations tested (Figure 1A), suggesting a lag phase. We calculated the initial velocity, V_0, which corresponds to the lag phase (using the data points from the first 250 s, Figure 1B−D), and the steady-state velocity, V_{ss}, which corresponds to the exponential phase (using the data points that give the maximal slope around 750−1250 s, Figure 1A−C). Zw12-PgtE showed a maximum steady-state velocity ($V_{max,ss}$) of 54.85 ± 3.43 nM s^{-1}, which is 6 times higher than the maximum initial velocity ($V_{max,0}$), which is about 8.61 ± 0.30 nM s^{-1}. The disparity between V_0 and V_{ss} suggests a non-Michaelis−Menten, hysteretic enzymatic behavior,[39−41] which characterizes a kinetic transition usually associated with a slow conformational change before an enzyme attains the linear steady state kinetics, in response to an increase in substrate concentration. In the case of Zw12-PgtE, this transition was accompanied by an increase in k_{cat} (0.0043 to 0.027 s^{-1}).

To rule out that this is not due to a suboptimal, non-native conformational state[42,43] of the PgtE due to the micellar scaffold or nonoptimal selection of detergent (as Zw12 was optimized for OmpT[38]), we measured the *in situ* activity of endogenous PgtE overexpressed on the outer membrane of the *E. coli* BL21 ΔABCF strain, which lacks main *E. coli* OMPs (LamB, OmpA, OmpC, and OmpF). Similarly, a clear lag phase was evident in the progress curve (Figure S4A). The similarity in the kinetic profiles suggests that PgtE in the Zw12 micelle had adopted a folded conformation with a native-like kinetic profile and this is indicative of potential physiological significance. Interestingly, when we compared the activity of Zw12-PgtE to that of Zw12-stabilized OmpT in a similar assay condition, no hysteresis was found for the latter (Figure S4B), consistent with previous reports.[37,38,44]

This adds to a slow growing list of hysteretic enzymes,[45] but with a twist: the hysteretic enzymatic behavior is associated with regulatory metabolic enzymes[40,45−47] that purportedly "damp" the spontaneous fluctuation in ligand concentration.[40] In comparison, PgtE is thought to function efficiently in its protective response against the instantaneous rise in antimicrobial peptide concentration and a multitude of physiological functions.[23] The contrasting physiological function of PgtE with that of the known hysteretic enzymes reveals a previously unexplored functional category and expands the scope of hysteretic enzymatic behavior.

Factors Affecting the Hysteretic Behavior of Zw12-PgtE

We sought to determine whether the hysteretic behavior of Zw12-PgtE can be altered. The protease assay was typically performed with a 15 min preincubation of Zw12-PgtE with LPS to initiate the binding of LPS (Figure 2A, black line), considering its importance for omptin activity.[34,35,37,38] We questioned whether substrate binding alone may prime the protease and induce rapid attainment of the steady state. To test this idea, the 15 min LPS preincubation was replaced with a 10 min substrate preincubation, followed by the addition of LPS to activate the proteolytic process (Figure 2A, red line). During the preincubation (before the addition of LPS), the substrate was not cleaved (data not shown). Surprisingly, the reversal—sequential addition of substrate and LPS—abolished the hysteresis (Figure 2A, red line), achieving $V_{max,0}$ of 50.49 nM s^{-1} rapidly within the first hundreds of seconds (Figure 2B), matching the $V_{max,ss}$ of a typical reaction performed with the LPS preincubation step (54.85 nM s^{-1}). Furthermore, a similar k_{cat} of 0.025 s^{-1} was achieved. The induction period, which is the time taken for the enzyme to reach its steady state, was found to reduce drastically from hundreds of seconds to less than 30 s for substrate concentration up to 500 μM (Figure 2C). These results suggest that the availability of substrate, rather than LPS, converts PgtE into a preactive [PgtE-substrate] state, which undergoes rapid conformational transition into a fully active state when LPS is available and converts substrate to product without substantial delay.

The existence of a preactive [PgtE-substrate] state was supported by our preliminary structural analyses based on far-ultraviolet circular dichroism (CD) spectroscopy (Figure S5) and Tyr/Trp fluorescence spectroscopy (Figure S6). A slight change in the CD spectra of Zw12-PgtE was observed when the protein was mixed with the substrate in the absence of LPS (Figure S5). The largely similar spectra and the lack of a dose-dependent effect with increasing amounts of the substrates are indicative of an absence of major structural change. In the Tyr/Trp fluorescence analysis, when Zw12-PgtE and the substrate were mixed and the solution was excited at 280 or 295 nm, the intensity of the emission peak around 340 nm was reduced (data not shown), suggesting conformational changes or Förster resonance energy transfer (FRET) from the Trp residues to the substrate. Because the peptide substrate (Abz-ARRA-Tyr(NO_2)-NH_2) was quenched when not cleaved, the lack of emission from the peptide precluded the conclusion. To further test the occurrence of FRET events, we synthesized a fluorescent peptide (Abz-AR) which absorbs weakly at the two excitation wavelengths and as a result emits only weakly at 420 nm when FRET-ting is absent. Indeed, when the Abz-AR peptide was mixed and the solution was excited at 280 or 295 nm, two peaks around 340 and 420 nm, which correspond to the emission maxima of Tyr/Trp and Abz, respectively, were observed (Figure S6A,B). The result showed a reduction in the intensity at 340 nm and an increase in the intensity at 420 nm with an increasing amount of Abz-AR peptide, confirming that FRET from Trp residues to the substrate (Abz-AR) has occurred.[48,49] Further comparison to the emission spectrum of Abz-AR alone validated this interpretation. If there is no coupling of the Abz-AR peptide to Zw12-PgtE in the mixture, the emission intensities at 340 and 420 nm will be equal to the sum of Abz-AR and Zw12-PgtE measured separately, *i.e.*, (PgtE + Abz-AR) = (PgtE) + (Abz-AR). In our measurements, (PgtE + Abz-AR) intensities were less than the sum of independent measurements, *i.e.*, (PgtE + Abz) < (PgtE) + (Abz-AR) (Figure S6C,D), which supports the notion that Tyr/Trp residues in PgtE and Abz-AR are in proximity. The results thus suggest that a putative [PgtE-substrate] state exists.

https://doi.org/10.1021/acsbiomedchemau.1c00027
ACS Bio Med Chem Au 2022, 2, 73−83

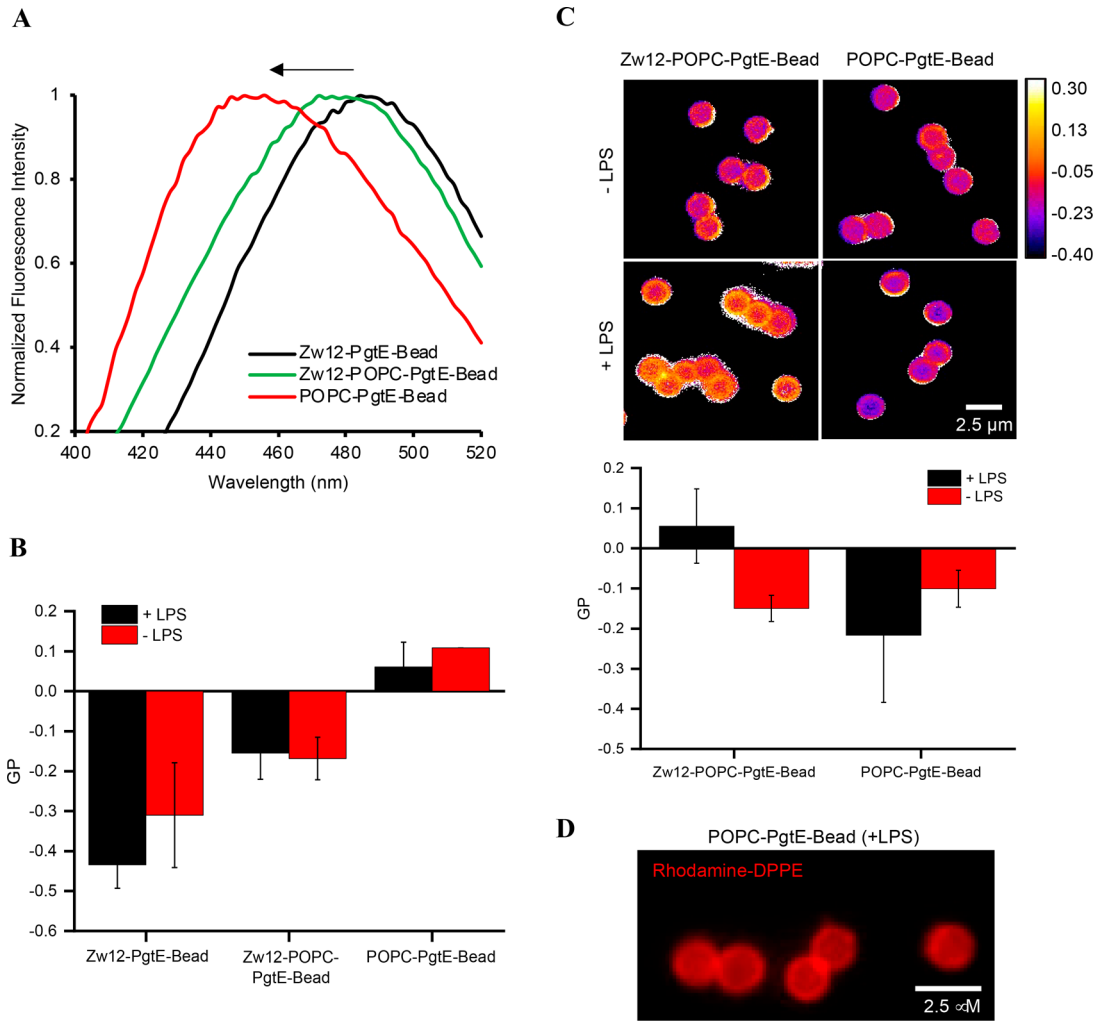

Figure 3. Formation of POPC bilayer on PgtE-conjugated silica beads. (A,B) Laurdan spectroscopy. (A) Normalized fluorescence emission spectra of Laurdan for PgtE-Bead reconstituted in different amphiphilic environments: detergent (Zw-12-PgtE-Bead), POPC bilayer without removal of detergent (Zw-12-POPC-PgtE-Bead), and POPC bilayer with removal of detergent using biobeads (POPC-PgtE-Bead). Spectra for the corresponding LPS-containing conditions are largely unchanged (not shown). (B) Generalized polarization (GP) calculation from (A). Error bars indicate the standard error for two independent measurements. (C) Top: Representative wide-field microscopy images of Laurdan-doped Zw12-POPC-PgtE-Bead and POPC-PgtE-Bead, with and without LPS. The color bar is calibrated based on the generalized polarization (GP) values. Bottom: Average GP value calculated from the image above. Error bars indicate the standard error for two independent measurements. (D) Representative wide-field microscopy image of POPC-PgtE-Bead (+LPS) doped with 0.5 mol % of Rhodamine-DPPE. POPC-PgtE-Bead shows a virtually identical fluorescence image.

Furthermore, we questioned if an activated enzyme may remain in the steady state conformation even after substrate depletion. In a separate permutation, new substrate was added to an enzymatic reaction that has ceased due the depletion of substrate. We find a disappearance of the lag phase for the second substrate addition step (Figure 2D), suggesting an inherent mnemonic property of activated Zw12-PgtE. This mnemonical characteristic allows the hysteretic enzyme to "remember" the active conformation induced by the binding of a substrate and remain active even after product dissociation, thus eliminating the lag phase.[40,41]

Taken together, the results show that LPS is essential for Zw12-PgtE to be active. The enzymatic behavior of PgtE can be tuned with substrate or cofactor (LPS) pre-exposure, which primes PgtE to adopt (i) a preactive [PgtE-substrate] state that can be readily activated with the availability of LPS, (ii) an inactive [PgtE-LPS] state that exhibits hysteretic behavior with the availability of substrate, or (iii) a fully active mnemonic [PgtE-LPS] state. While the existing data do not suggest major structural changes, we propose that the binding of the substrate in the absence of LPS induces subtle conformational changes in the vicinity of the substrate binding site that facilitate rapid activation of the protein.

Reconstitution of PgtE on Bead-Supported Amphiphilic Environments

The change in the enzymatic behavior due to inactive substrate binding prompts a further question: Does an amphiphilic environment, largely shown to influence protein folding,[1,2,10] also alter the enzymatic behavior? We compared the proteolytic activity of PgtE stabilized in detergent micelles or a phospholipid bilayer. A change in the apparent activity of a membrane protein within a specific solubilizing environment may be influenced by the physicochemical properties of the environment, or it may arise simply from a difference in the amount of reconstituted membrane protein within the target environment. The latter has to be ruled out for meaningful

https://doi.org/10.1021/acsbiomedchemau.1c00027
ACS Bio Med Chem Au 2022, 2, 73−83

discussion of any change in the apparent protein activity when different environments are considered. For that, complete reconstitution of Zw12-PgtE into a bilayer environment needs to be ascertained. Our strategy is first to conjugate Zw12-PgtE onto Ni^{2+}-nitrilotriacetate (NTA)-functionalized silica beads (1.5 μm in diameter), followed by substitution of the surrounding detergent micelles with phospholipids, inspired by methods reported previously.[50,51]

Zw12-PgtE was conjugated onto the beads based on polyhistidine-Ni^{2+} interaction. The beads that were conjugated with Zw12-PgtE were referred to as Zw12-PgtE-Bead. A series of conditions, which include the incubation duration, incubation and wash buffers, as well as bead-to-protein ratio, were tested to ensure 100% binding efficiency. For validation of binding efficiency, the samples from each step (total protein load, unbound protein in the supernatant after centrifugation of protein-bound beads, two washes, and elution with 500 mM imidazole) were loaded onto SDS-PAGE gel. No protein band was detected in the unbound fraction (Figure S7A), and the thickness of the protein bands in the elution was similar to that in the load, thus indicating that 100% of the protein was conjugated to the beads. Furthermore, Zw12-PgtE and Zw12-PgtE-Bead showed similar activity, indicating that bead immobilization does not affect the protease activity (Figure S7B).

Next, we reconstituted PgtE into two membrane environments: a mixed detergent-phospholipid bilayer and a phospholipid bilayer. Small POPC unilamellar vesicles (SUVs, ~100 nm) were first added to Zw12-PgtE-Bead along with a critical micellar concentration (CMC) equivalent (2 mM) of Zw12 detergent. The sample at this stage consisted of mixed detergent−phospholipid bilayer on the beads and was referred to as Zw12-POPC-PgtE-Bead. When an excess amount of detergent (~10× CMC) was used during the incubation with POPC SUVs, as described by Zheng *et al.*,[50] a low activity of PgtE was detected (Figure S8), and therefore, this method was not used for further experiments. Detergent removal using Bio-Beads was performed on Zw12-POPC-PgtE-Bead to obtain a detergent-free PgtE stabilized in a bilayer structure (POPC-PgtE-Bead). Additional LPS-containing variants were produced by supplementing LPS before the incubation of POPC SUV and Zw12-PgtE-Bead. The POPC bilayer formed in the absence of a CMC equivalent amount of Zw12 detergent gave rise to inactive PgtE. Similarly, the protein was inactive when Zw12-PgtE-Bead was assayed in a detergent-free buffer. This is presumably due to the rapid dissociation of detergent micelles from bead-bound PgtE in response to the depletion of detergent in the bulk phase, leading to the unfolding of the protein. This further suggests that, during the repeated Bio-Beads washes, the majority of Zw12 had been removed and residual Zw12 did not contribute to the activity measured.

The proper formation of a POPC bilayer was supported by Laurdan spectroscopy and microscopy. A blue-shift of the emission peak maximum from 490 nm (Zw12-PgtE-Bead) to 440 nm (POPC-PgtE-Bead) was observed, accompanied by an increase in the absolute emission intensity, consistent with a reduction in the polarity of the Laurdan environment in the interfacial headgroup-tail region in POPC relative to Zw12 environment[52] (Figure 3A). A generalized polarization (GP) value of about 0.1 was obtained for POPC-PgtE-Bead (Figure 3B), in agreement with reported values.[53] Zw12-PgtE-Bead showed a GP of around −0.4, while Zw12-POPC-PgtE-Bead with the hybrid detergent−phospholipid composition showed an intermediate value of about −0.15. The emission was contributed by the amphipile-coated beads but not from the free amphiphile in the exterior bath, as confirmed by microscopy analysis of the Laurdan-loaded bead samples (Figure 3C). Clear Laurdan fluorescence localized on the beads was detected, and similar GP values were obtained in the microscopy analysis. Furthermore, when we doped POPC SUV with 0.5 mol % 1,2-dipalmitoyl-*sn*-glycero-3-phosphoethanolamine-*N*-(lissamine rhodamine B sulfonyl) (Rhod-DPPE), an intense and largely homogeneous ring-shaped structure around the beads was observed under a wide-field fluorescence microscope, which suggests the presence of a bead-supported phospholipid membrane (Figure 3D). The substantial activity obtained for this sample (shown in the next section) further supports that a single POPC membrane was formed around the protein, which allows the extracellular domain of PgtE to be used for substrate cleavage. The inclusion of LPS did not significantly alter the Laurdan nor Rhod-DPPE signals (Figure 3B,C).

Comparison of PgtE Activity in the Micelles and Phospholipid Bilayer

The enzymatic activities of Zw12-PgtE-Bead, Zw12-POPC-PgtE-Bead, and POPC-PgtE-Bead were measured using identical assay conditions as above, in the absence or presence of LPS (Figure 4A). Zw12-PgtE-Bead (+LPS) and Zw12-PgtE-Bead were used as positive and negative controls, respectively. Several noteworthy results were obtained. First, the activity of PgtE was similar in micellar and bilayer environments, as shown by Zw12-PgtE-Bead (+LPS), Zw12-POPC-PgtE-Bead (+LPS), and POPC-PgtE-Bead (+LPS) (Figure 4B, dark bars of A, C, E). Second, PgtE reconstituted in POPC bilayer showed substantial activity in the absence of LPS (about 70% activity of the positive control) (Figure 4B, dark bars of A, B, D, F). To our knowledge, this is the first account of LPS-independent protease activity for members in the omptin family[10,23,34,35,38,54] and contrasts the findings from other reports on PgtE.[24,35] Third, the hysteresis behavior that characterizes the PgtE stabilized in the micellar environment (Zw12-PgtE-Bead) was abolished in the bilayer environment (POPC-PgtE-Bead) where the initial velocity equals the steady state velocity (Figure 4B, dark bar of A, F). The initial velocity of PgtE-Bead reconstituted in POPC bilayer significantly increased by ~200% compared to that in the micellar environment. The effect on the enhanced initial velocity was also noted for the other POPC-containing environments, but a consistent gap between the initial and steady state velocities exists, suggesting residual hysteresis (Figure 4B, dark bars of C−E).

A correlation in the packing order of amphiphiles and the initial or steady state velocities of PgtE is noted (Figures 3B and 4B). We rationalize that the structure of PgtE embedded in a micellar environment exhibits high flexibility, especially at the micellar headgroup region.[55,56] In this environment, LPS is needed, presumably to reduce the excessive conformational flexibility.[34] For the mixed detergent/POPC environment, the presence of POPC offers sufficient restraint in mobility that LPS is now rendered nonessential, despite its positive effect on activity. For the POPC environment, PgtE is stably positioned within a relatively ordered surrounding and is readily activated with substrate availability. The addition of LPS in this case does not improve the enzymatic function; if anything, the

https://doi.org/10.1021/acsbiomedchemau.1c00027
ACS Bio Med Chem Au 2022, 2, 73−83

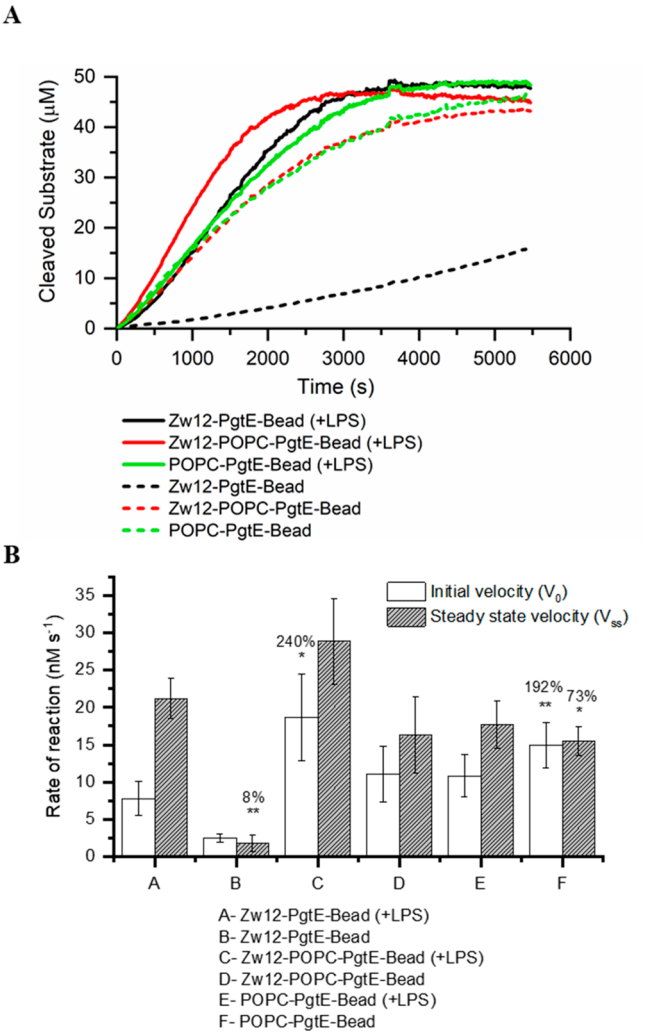

Figure 4. Enzymatic activity of PgtE-Bead reconstituted in different amphiphilic environment, in presence and absence of LPS. (A) Average progress curves of PgtE-Bead reconstituted in a POPC bilayer under CMC level detergent (2 mM $DodMe_2NPrSO_3$, 20 mM Bis-Tris, 5 mM EDTA, pH 6), with and without removal of the detergent. (B) Bar chart representing the rate of reaction of PgtE-Bead reconstituted in different amphiphilic environments: detergent (conditions A and B), POPC bilayer without 2 mM detergent removal (conditions C and D), and POPC bilayer with 2 mM detergent removal (conditions E and F). Enzymatic activity was compared with detergent stabilized PgtE-Bead in the presence of LPS (condition A). $*p < 0.05$; $**p < 0.01$. The values above the bars refer to the percentage of activity relative to that of condition A. Error bars indicate the standard deviation for five independent measurements.

enzymatic function is reduced (Figure 4B, white bar of E). LPS is known to disrupt the bilayer organization[57] and, in agreement with our result, causes a reduction in enzymatic function.

CONCLUSION

In this study, we detailed the production of PgtE and compared the proteolytic activity of PgtE as a function of its solubilizing environments, namely, detergent micelles, mixed detergent-phospholipid structure, and phospholipid bilayer, in the presence or absence of LPS. Similar activity was detected for PgtE stabilized in the micellar or lipid bilayer environments, which suggests that bilayer-specific physical parameters,[58] such as lateral pressure and chain ordering gradients, membrane curvature, and membrane bending stress, may not be critical for the activation of PgtE. Rather, factors that may be critical in regulating the enzymatic efficiency of PgtE include the unique lipid packing of the outer membrane, substrate, or LPS availability. Strikingly, the presumably equimolar binding of LPS for PgtE activation becomes nonessential when the protein is reconstituted into a POPC bilayer. While its physiological significance remains to be examined, it is tempting to speculate that, within the protein-rich outer membrane, direct binding to LPS may modulate, rather than activate, the protease. These findings suggest numerous biological nuances for PgtE that have not been well appreciated and raise new perspectives that may generally be applicable for omptin family of proteases.

MATERIALS AND METHODS

Materials

The plasmids, pgtE_pET28a and sp_pgtE_pET28a, and *E. coli* BL21(DE3) were prepared by Dr. Gaurav Sinsinber (Nanyang Technological University, Singapore). The plasmids were synthesized and sequenced by Bio Basic Inc. (Singapore). *E. coli* BL21 ΔABCF was a gift from the Jack Leo Lab (Bacterial strain #102270). Luria–Bertani (LB) broth was purchased from BD Difco (Franklin Lakes, NJ, USA). Kanamycin was purchased from Thermo Fisher Scientific (Waltham, MA, USA). Isopropyl thio-*β*-D-galactopyranoside (IPTG) was purchased from Gold Biotechnology (St. Louis, MO, USA). Zwittergent 3-12 (*N*-dodecyl-N,*N*-dimethyl-3-ammonio-1-propanesulfonate, Zw12) and lipopolysaccharides (LPS) from *E. coli* 0111:B4 purified by phenol extraction, Corning Black, clear flat bottom 96-well plates, HIS-Select Cobalt Affinity Gel, and 6-dodecanoyl-*N*,*N*-dimethyl-2-naphthylamine (Laurdan) were purchased from Sigma-Aldrich (Singapore). TALON Metal Affinity Resin charged with cobalt was purchased from Takara Bio (Kusatsu, Shiga, Japan). Urea was purchased from Affymetrix USB (Santa Clara, CA, USA). PD-10 Desalting Columns containing Sephadex G-25 resin were purchased from GE Healthcare Life Sciences (Singapore). DiagNano Ni-NTA Silica Particles of 1.5 μm in diameter were purchased from Creative Diagnostics (Shirley, NY, USA). 1-Palmitoyl-2-oleoyl-glycero-3-phosphocholine (POPC) and 1,2-dipalmitoyl-*sn*-glycero-3-phosphoethanolamine-*N*-(lissamine rhodamine B sulfonyl) (Rho-DPPE) were obtained from Avanti Polar Lipids (Alabaster, AL, USA). Bio-Beads SM-2 were acquired from Bio-Rad Laboratories (Singapore). Synthetic peptide, Abz-ARRA-Tyr(NO_2)-NH_2, and Abz-AR-NH_2 were purchased as lyophilized powders and certified as having >95% purity from Biomatik (Cambridge, ON, Canada).

Overexpression, Purification, and Refolding of Recombinant PgtE

The plasmid pgtE_pET28a consists of the mature PgtE sequence without the signal sequence (275 residues) in addition to a hexahistidine sequence at the N-terminal and a linker sequence, GSGSGSGS. pgtE_pET28a was transformed into *E. coli* BL21(DE3). Hexahistidine-tagged PgtE (PgtE) was expressed as inclusion bodies (IBs) in *E. coli* BL21(DE3) cells following a method previously described,[37] with some modifications. Briefly, the transformed *E. coli* BL21(DE3) cells were inoculated in 5 × 10 mL LB broth and incubated overnight with 50 μg/mL kanamycin at 37 °C and swirled at 220 rpm in a shaking incubator. Then 50 mL of primary culture was inoculated into 1 L of LB broth supplemented with 50 μg/mL kanamycin to produce secondary cultures. IPTG (1 mM) was added to the secondary culture when OD600 reached ∼0.6 for induction at 37 °C for 4 h. After induction, the cells were harvested and washed with 1× phosphate-buffered saline (PBS), pH 7.4 before resuspending the pellet in 20 mL of lysis buffer (50 mM Tris-HCl, 40 mM EDTA, pH 8.0). These cells were kept on ice for 20 min before adding a further 20 mL of prechilled lysis buffer, followed by a second

https://doi.org/10.1021/acsbiomedchemau.1c00027
ACS Bio Med Chem Au 2022, 2, 73–83

incubation on ice for 20 min. After lysis buffer treatment, the cells were sonicated with Sonics a Vibra cell VCX-130 instrument (Sonics & Materials INC., USA) for 50 min (2 s on, 6 s off, and 60% amplitude), in which the solution turned clearer. The lysate was centrifuged at 4500*g* for 30 min to pellet the IBs, which was then washed twice with 60 mL of PBS. The IBs were solubilized in 10 of mL solubilizing buffer (150 mM NaCl, 8 M urea, 0.1 M sodium phosphate, pH 8.3) and kept on ice for 3−4 h with intermittent shaking. The solubilized IBs were centrifuged at 10 000*g* for 10 min to pellet the protein aggregates, and the supernatant was collected as a nonpurified PgtE fraction.

The extracted PgtE was further purified using TALON Metal Affinity Resin. In brief, the resin was first equilibrated with 10 column volumes (CV) of solubilizing buffer, followed by the addition of the nonpurified PgtE sample to the resin and gentle agitation at room temperature for 30 min on a platform shaker. After 30 min of incubation, the resin was washed with 5 CV of 10 mM imidazole, followed with 5 CV of 200 mM Imidazole for elution. The eluate was collected in 2 mL per fraction and was analyzed for purity using SDS-PAGE. The fractions were pooled together before proceeding with imidazole removal using PD-10 columns. PD-10 columns were first equilibrated with solubilizing buffer, followed by loading of the affinity-purified PgtE into the column, and imidazole-free, purified fractions were collected. For refolding, the purified PgtE was added to prechilled refolding buffer (20 mM Tris-HCl, 31 mM Zw12, pH 7.5) in the ratio of 1:50 (20 μL IBs and 980 μL RB) and incubated for 3−4 h on ice. The sample was aliquoted and stored at −20 °C for further use. The refolded PgtE was referred to as Zw12-PgtE. The concentration of purified PgtE samples was estimated using the NanoDrop 2000c spectrophotometer (ThermoFischer Scientific, Singapore) using a molar absorption coefficient of 78 270 M^{-1} cm^{-1}. To confirm the identity of the purified PgtE, the sample was analyzed using MALDI-TOF/TOF and LC-MS/MS. The purified PgtE sample was prepared for LC-MS/MS analysis using methanol/chloroform/water precipitation to remove the detergent.[38] Subsequently, the sample was resuspended in 5% acetonitrile and 0.1% formic acid in water to a concentration of 15 μ M and submitted for analysis (NTU/SBS proteomics core facility). Three protein bands were excised from the SDS-PAGE gel and submitted for MALDI-TOF/TOF mass spectrometry analysis (NTU/SBS proteomics core facility).

Overexpression of Outer-Membrane Embedded PgtE

The sp_pgtE_pET28a consisting of the precursor PgtE sequence with an intact signal sequence (312 residues) was transformed into *E. coli* BL21 ΔABCF, which lacks main *E. coli* OMPs (LamB, OmpA, OmpC, and OmpF). The transformed *E. coli* cells were inoculated in 10 mL of low salt LB broth (10 g/L tryptone, 5 g/L yeast, 5g/L NaCl) and incubated overnight with 50 μg/mL kanamycin at 37 °C and swirled at 220 rpm in a shaking incubator. Then 10 mL of primary culture was inoculated into 200 mL of low salt LB broth supplemented with 50 μg/mL kanamycin to produce secondary cultures. IPTG (0.4 mM) was added to the secondary culture when OD600 reached ∼0.6 for induction at 37 °C for 3 h. After induction, the cells were harvested and washed with 1× PBS, pH 7.4 before resuspending the pellet in 20 mL of lysis buffer (50 mM Tris-HCl, 40 mM EDTA, pH 8.0).

Small Unilamellar Vesicle (SUV) Preparation

Desired amounts of POPC in chloroform with or without 0.5 mol % Rho-DPPE were added to a glass tube. The chloroform was evaporated under nitrogen gas and further dried under vacuum for 1 h. The dried lipid films were then rehydrated in PBS by brief vortexing and stirred for 30 min to obtain multilamellar vesicle suspensions at 4 mg/mL. The vesicle suspensions were subsequently extruded 21 times using an Avanti Mini-Extruder (Avanti Polar Lipids, Alabaster, AL, USA) at room temperature (∼22 °C). The extruder was assembled with a 100 nm polycarbonate membrane, two filter supports, and two 1 mL gastight syringes from Hamilton (Reno, NV, USA). The SUVs were used immediately or stored at 4 °C. The hydrodynamic size of the SUVs was validated using a Zetasizer Nano ZS instrument (Malvern Panalytical, Malvern, UK).

Reconstitution of Bead Supported PgtE in Different Amphiphilic Environments

PgtE was reconstituted in six bead-supported amphiphilic environments: (i) Zw12 detergent (Zw12-PgtE-Bead); (ii) POPC bilayer without removal of detergent (Zw12-POPC-PgtE-Bead); (iii) POPC bilayer with removal of detergent using Bio-Beads (POPC-PgtE-Bead); (iv) Zw12 detergent supplemented with LPS (Zw12-PgtE-Bead(+LPS)); (v) POPC bilayer without removal of detergent supplemented with LPS (Zw12-POPC-PgtE-Bead(+LPS)); (vi) POPC bilayer with removal of detergent using Bio-Beads and supplemented with LPS (POPC-PgtE-Bead(+LPS)). For Zw12-PgtE-Bead, 5 μL of stock Zw12-PgtE (14.81 μM) was added to 18 μL of Ni-NTA silica beads (excess solution in the beads removed) in a tube with assay buffer (20 mM Bis-tris, 2 mM Zw12, 5 mM EDTA, pH 6) added to a final volume of 50 μL. This mixture was incubated for 30 min for binding, followed by washing the beads twice with assay buffer to remove any free protein. The beads were then resuspended in 90 μL of assay buffer. The resultant sample was referred to as Zw12-PgtE-Bead. The binding efficiency of His-tagged PgtE to the beads was validated by tracking the amount of free PgtE in the supernatant in each step using SDS-PAGE and absorption at 280 nm (not shown) (Figure S7). For Zw12-PgtE-Bead(+LPS), Zw12-PgtE-Bead was incubated with 10 μg/mL LPS for 15 min, followed by subsequent steps as described below.

For environments with a bilayer, POPC SUVs was added to Zw12-PgtE-Bead and Zw-12-PgtE-Bead(+LPS) mixtures to a final concentration of 0.2 mg/mL POPC in a total volume of 300 μL and incubated for 15 min for bilayer formation. The resulting samples at this step were referred to as Zw12-POPC-PgtE-Bead and Zw12-POPC-PgtE-Bead(+LPS). The detergent in the two samples was removed with Bio-Beads to obtain POPC-PgtE-Bead and POPC-PgtE-Bead(+LPS). Briefly, 30 mg of Bio-Beads was added to the mixture for 30 min and then replaced with 15 mg of fresh Bio-Beads for subsequent 30 min. This stepwise removal of detergent was previously found to be critical for bilayer formation around the beads.[50] The samples without and with Bio-Beads treatment were then washed twice with detergent containing assay buffer (20 mM Bis-tris, 2 mM Zw12, 5 mM EDTA, pH 6) and nondetergent containing buffer (20 mM Bis-tris, 5 mM EDTA, pH 6), respectively, to remove excess free POPC vesicles. After washing, the beads were resuspended in 90 μL of their respective buffer and used for activity assay immediately. To confirm that the reconstitution was successful, the presence of the POPC membrane was determined based on fluorescence microscopy and Lauran spectroscopy (Figure 3).

PgtE Protease Activity Assay

The protease activity assay of PgtE was performed as described for OmpT by Sinsinbar *et al.*[37] with modifications. All fluorescence assays were performed in 96-well black with clear flat bottom polystyrene plates at a final reaction volume of 100 μL. Stocks of 500 μM synthetic peptide substrate Abz-ARRA-Tyr(NO2)-NH2 (ARRA) were prepared in in Milli-Q water. An extinction coefficient of 2200 M^{-1} cm^{-1} at 381 nm was used for concentration estimation. The stock solution of 2 mg/mL of LPS was prepared by dissolving LPS powder from *E. coli* O111:B4 in Milli-Q-water.

For free detergent stabilized PgtE samples, 13.5 μL of 14.81 μM Zw12-PgtE was first incubated with 0.5 μL of 2 mg/mL LPS for 15 min, followed by adding 76 μL of assay buffer and 10 μL of ARRA peptide stock to the mixture, resulting in a sample with a final concentration of 2 μM Zw12-PgtE with 10 μg/mL LPS and 50 μM Abz-ARRA peptide for the assay. For bead-supported detergent stabilized PgtE samples containing LPS, 90 μL of Zw12-PgtE-Bead was incubated with 0.5 μL of 2 mg/mL LPS for 15 min, followed by the addition of 10 μL of ARRA peptide stock, resulting in a final concentration of 0.74 μM PgtE with 10 μg/mL LPS and 50 μM ARRA. LPS was omitted for bead-supported detergent stabilized PgtE samples without LPS. For PgtE-Bead reconstituted in POPC bilayer

https://doi.org/10.1021/acsbiomedchemau.1c00027
ACS Bio Med Chem Au 2022, 2, 73−83

samples, 90 μL of Zw12-POPC-PgtE-Bead, Zw12-POPC-PgtE-Bead(+LPS), POPC-PgtE-Bead, and POPC-PgtE-Bead(+LPS) samples was added to 10 μL of ARRA peptide stock (final concentration of 0.74 μM PgtE, 18 μL of beads, 0.2 mg/mL POPC, with or without 10 μg/mL LPS and 50 μM Abz-ARRA).

All enzymatic reactions were performed at 37 °C with a preheated TECAN Spark multimode microplate reader (Männedorf, Switzerland). Fluorescence intensity were collected every 10 s for 60−120 min with the excitation wavelength set to 325 nm and emission at 420 nm. For samples with beads, interval shaking of 72 rpm was set for every 150 s of fluorescence measurement to prevent settling of the beads that affects the reading. The data was plotted and kinetic parameters were calculated in OriginPro 9.1. Results are presented as mean ± SD. Statistical analysis was performed using paired Student's *t* test, with $*p < 0.05$ and $**p < 0.01$.

Laurdan Spectroscopy

The Laurdan stock solution (1 mM) was prepared by dissolving the powder stocks in methanol and then was either used fresh or stored at −20 °C. To obtain a final concentration of 10 μM Laurdan, 1 μL of stock Laurdan was mixed with 99 μL of bead samples (from previous section). Spectroscopic measurements were performed on a TECAN Spark multimode microplate reader (Männedorf, Switzerland) using a 96-well black with clear flat bottom polystyrene plate (Corning Inc., Tewksbury, MA, USA). An excitation wavelength of 340 nm was used, and emission wavelengths from 400 to 520 nm were collected. For G) calculations, the following equation was used:

$$\mathrm{GP} = \frac{I_{440} - I_{490}}{I_{440} + I_{490}}$$

where I_{440} and I_{490} refer to the steady state intensities at 440 and 490 nm, respectively.

Wide-Field Fluorescence Microscopy

Wide-field fluorescence microscopy images were acquired on a DeltaVision microscope (Applied Precision Inc., Issaquah, WA, USA) fitted with a PLAPON 60XO/1.42 NA oil-immersion objective from Olympus (Shinjuku-ku, Tokyo, Japan), with DAPI (4′,6-diamidino-2-phenylindole), TRITC (tetramethylrhodamine isothiocyanate), and FITC (fluorescein isothiocyanate) Semrock filters (New York, NY, USA), and a mercury lamp (Intensilight C-HGFIE, Nikon Corporation, Tokyo, Japan). Images were processed in Fiji ImageJ.[59]

For Laurdan microscopy, two-channel images were acquired using two designated filter sets (DAPI/DAPI and DAPI/FITC) with identical exposure settings. GP analysis of the images were performed in Fiji ImageJ based on the following format:

$$\mathrm{GP} = \frac{\mathrm{image}_{\mathrm{DAPI/DAPI}} - \mathrm{image}_{\mathrm{DAPI/FITC}}}{\mathrm{image}_{\mathrm{DAPI/DAPI}} + \mathrm{image}_{\mathrm{DAPI/FITC}}}$$

where $\mathrm{image}_{\mathrm{DAPI/DAPI}}$ and $\mathrm{image}_{\mathrm{dapi/FITC}}$ refer to images acquired using DAPI/DAPI and DAPI/FITC filter sets, respectively, following the classical equation.

Tyrosine and Tryptophan Fluorescence Spectroscopy

Fluorescence emission scans (Ex = 295 or 280 nm, Em = 320−480 nm) were collected for the bead samples, prepared as described above. Spectroscopic measurements were performed on a TECAN Spark multimode microplate reader (Männedorf, Switzerland) using a 96-well black with clear flat bottom polystyrene plate (Corning Inc., Tewksbury, USA). Data presented were from two or three independent samples.

Safety Statement

No unexpected or unusually high safety hazards were encountered.

ASSOCIATED CONTENT

Supporting Information

The Supporting Information is available free of charge at https://pubs.acs.org/doi/10.1021/acsbiomedchemau.1c00027.

LC-MS/MS, SDS-PAGE, and MALDI-TOF/TOF mass spectrometry analyses of purified PgtE; optimization of protease assay conditions; enzymatic behavior of native PgtE overexpressed on *E. coli* outer membrane; enzymatic behavior of refolded OmpT, circular dichroism, and intrinsic fluorescence spectroscopic analyses; immobilization of PgtE on beads; optimization of reconstitution of Zw12-PgtE into POPC bilayer (PDF)

AUTHOR INFORMATION

Corresponding Author

Bo Liedberg − *Centre for Biomimetic Sensor Science, Nanyang Technological University, 637553, Singapore; School of Materials Science and Engineering, Nanyang Technological University, 639798, Singapore;* orcid.org/0000-0003-2883-6953; Email: bliedberg@ntu.edu.sg

Authors

Siau Ling Kum − *Centre for Biomimetic Sensor Science, Nanyang Technological University, 637553, Singapore; School of Materials Science and Engineering, Nanyang Technological University, 639798, Singapore*

James C. S. Ho − *Centre for Biomimetic Sensor Science, Nanyang Technological University, 637553, Singapore; School of Materials Science and Engineering, Nanyang Technological University, 639798, Singapore*

Atul N. Parikh − *Centre for Biomimetic Sensor Science, Nanyang Technological University, 637553, Singapore; School of Materials Science and Engineering, Nanyang Technological University, 639798, Singapore; Department of Chemistry and Department of Biomedical Engineering, University of California, Davis, California 95616, United States;* orcid.org/0000-0002-5927-4968

Complete contact information is available at: https://pubs.acs.org/10.1021/acsbiomedchemau.1c00027

Author Contributions

⊥S.L.K. and J.C.S.H.: Equal contribution to this work.

Notes

The authors declare no competing financial interest.

ACKNOWLEDGMENTS

We would like to acknowledge Dr. Sushanth Gudlur and Dr. Gaurav Sinsinbar for their helpful discussions. This research work was funded by the Singapore Ministry of Education Academic Research Fund Tier 2 (MOE2018-T2-1-025). S.L.K. is supported by the Provost Office, Nanyang Technological University and a grant from Lund University. J.H.C.S., A.N.P., and B.L. acknowledge the support from the Provost Office and the School of Materials Science & Engineering, Nanyang Technological University.

REFERENCES

(1) Cross, T. A.; Sharma, M.; Yi, M.; Zhou, H. X. Influence of solubilizing environments on membrane protein structures. *Trends Biochem. Sci.* **2011**, *36* (2), 117−25.

(2) Matthews, E. E.; Zoonens, M.; Engelman, D. M. Dynamic helix interactions in transmembrane signaling. *Cell* **2006**, *127* (3), 447−50.

(3) McMorran, L. M.; Brockwell, D. J.; Radford, S. E. Mechanistic studies of the biogenesis and folding of outer membrane proteins in vitro and in vivo: what have we learned to date? *Arch. Biochem. Biophys.* **2014**, *564*, 265−80.

(4) Wimley, W. C. The versatile beta-barrel membrane protein. *Curr. Opin. Struct. Biol.* **2003**, *13* (4), 404−11.

(5) Botos, I.; Noinaj, N.; Buchanan, S. K. Insertion of proteins and lipopolysaccharide into the bacterial outer membrane. *Philos. Trans. R. Soc., B* **2017**, *372* (1726), 20160224.

(6) Noinaj, N.; Kuszak, A. J.; Gumbart, J. C.; Lukacik, P.; Chang, H.; Easley, N. C.; Lithgow, T.; Buchanan, S. K. Structural insight into the biogenesis of beta-barrel membrane proteins. *Nature* **2013**, *501* (7467), 385−90.

(7) Paracini, N.; Clifton, L. A.; Skoda, M. W. A.; Lakey, J. H. Liquid crystalline bacterial outer membranes are critical for antibiotic susceptibility. *Proc. Natl. Acad. Sci. U. S. A.* **2018**, *115* (32), E7587−E7594.

(8) Nikaido, H. Molecular basis of bacterial outer membrane permeability revisited. *Microbiol. Mol. Biol. Rev.* **2003**, *67* (4), 593−656.

(9) Labischinski, H.; Barnickel, G.; Bradaczek, H.; Naumann, D.; Rietschel, E. T.; Giesbrecht, P. High state of order of isolated bacterial lipopolysaccharide and its possible contribution to the permeation barrier property of the outer membrane. *J. Bacteriol.* **1985**, *162* (1), 9−20.

(10) Horne, J. E.; Brockwell, D. J.; Radford, S. E. Role of the lipid bilayer in outer membrane protein folding in Gram-negative bacteria. *J. Biol. Chem.* **2020**, *295* (30), 10340−10367.

(11) Knol, J.; Sjollema, K.; Poolman, B. Detergent-mediated reconstitution of membrane proteins. *Biochemistry* **1998**, *37* (46), 16410−5.

(12) Rigaud, J. L.; Levy, D. Reconstitution of membrane proteins into liposomes. *Methods Enzymol.* **2003**, *372*, 65−86.

(13) Ritchie, T. K.; Grinkova, Y. V.; Bayburt, T. H.; Denisov, I. G.; Zolnerciks, J. K.; Atkins, W. M.; Sligar, S. G. Chapter 11 - Reconstitution of membrane proteins in phospholipid bilayer nanodiscs. *Methods Enzymol.* **2009**, *464*, 211−31.

(14) Tribet, C.; Audebert, R.; Popot, J. L. Amphipols: polymers that keep membrane proteins soluble in aqueous solutions. *Proc. Natl. Acad. Sci. U. S. A.* **1996**, *93* (26), 15047−50.

(15) Dorr, J. M.; Scheidelaar, S.; Koorengevel, M. C.; Dominguez, J. J.; Schafer, M.; van Walree, C. A.; Killian, J. A. The styrene-maleic acid copolymer: a versatile tool in membrane research. *Eur. Biophys. J.* **2016**, *45* (1), 3−21.

(16) Burgess, N. K.; Dao, T. P.; Stanley, A. M.; Fleming, K. G. Beta-barrel proteins that reside in the Escherichia coli outer membrane in vivo demonstrate varied folding behavior in vitro. *J. Biol. Chem.* **2008**, *283* (39), 26748−58.

(17) Katira, S.; Mandadapu, K. K.; Vaikuntanathan, S.; Smit, B.; Chandler, D. Pre-transition effects mediate forces of assembly between transmembrane proteins. *eLife* **2016**, *5*, No. e13150.

(18) Marsh, D. Energetics of hydrophobic matching in lipid-protein interactions. *Biophys. J.* **2008**, *94* (10), 3996−4013.

(19) Ramakrishnan, M.; Pocanschi, C. L.; Kleinschmidt, J. H.; Marsh, D. Association of spin-labeled lipids with beta-barrel proteins from the outer membrane of Escherichia coli. *Biochemistry* **2004**, *43* (37), 11630−6.

(20) Marsh, D.; Shanmugavadivu, B.; Kleinschmidt, J. H. Membrane elastic fluctuations and the insertion and tilt of beta-barrel proteins. *Biophys. J.* **2006**, *91* (1), 227−32.

(21) Goose, J. E.; Sansom, M. S. Reduced lateral mobility of lipids and proteins in crowded membranes. *PLoS Comput. Biol.* **2013**, *9* (4), No. e1003033.

(22) Anbazhagan, V.; Qu, J.; Kleinschmidt, J. H.; Marsh, D. Incorporation of outer membrane protein OmpG in lipid membranes: protein-lipid interactions and beta-barrel orientation. *Biochemistry* **2008**, *47* (23), 6189−98.

(23) Haiko, J.; Suomalainen, M.; Ojala, T.; Lahteenmaki, K.; Korhonen, T. K. Breaking barriers–attack on innate immune defences by omptin surface proteases of enterobacterial pathogens. *Innate Immun.* **2009**, *15* (2), 67−80.

(24) Lahteenmaki, K.; Kyllonen, P.; Partanen, L.; Korhonen, T. K. Antiprotease inactivation by Salmonella enterica released from infected macrophages. *Cell. Microbiol.* **2005**, *7* (4), 529−38.

(25) Yun, T. H.; Cott, J. E.; Tapping, R. I.; Slauch, J. M.; Morrissey, J. H. Proteolytic inactivation of tissue factor pathway inhibitor by bacterial omptins. *Blood* **2009**, *113* (5), 1139−48.

(26) Haiko, J.; Laakkonen, L.; Juuti, K.; Kalkkinen, N.; Korhonen, T. K. The omptins of Yersinia pestis and Salmonella enterica cleave the reactive center loop of plasminogen activator inhibitor 1. *J. Bacteriol.* **2010**, *192* (18), 4553−61.

(27) Valls Seron, M.; Haiko, J.; De Groot, P. G.; Korhonen, T. K.; Meijers, J. C. Thrombin-activatable fibrinolysis inhibitor is degraded by Salmonella enterica and Yersinia pestis. *J. Thromb. Haemostasis* **2010**, *8* (10), 2232−40.

(28) Jarvinen, H. M.; Laakkonen, L.; Haiko, J.; Johansson, T.; Juuti, K.; Suomalainen, M.; Buchrieser, C.; Kalkkinen, N.; Korhonen, T. K. Human single-chain urokinase is activated by the omptins PgtE of Salmonella enterica and Pla of Yersinia pestis despite mutations of active site residues. *Mol. Microbiol.* **2013**, *89* (3), 507−17.

(29) Ramu, P.; Tanskanen, R.; Holmberg, M.; Lahteenmaki, K.; Korhonen, T. K.; Meri, S. The surface protease PgtE of Salmonella enterica affects complement activity by proteolytically cleaving C3b, C4b and C5. *FEBS Lett.* **2007**, *581* (9), 1716−20.

(30) Riva, R.; Korhonen, T. K.; Meri, S. The outer membrane protease PgtE of Salmonella enterica interferes with the alternative complement pathway by cleaving factors B and H. *Front. Microbiol.* **2015**, *6*, 63.

(31) Ramu, P.; Lobo, L. A.; Kukkonen, M.; Bjur, E.; Suomalainen, M.; Raukola, H.; Miettinen, M.; Julkunen, I.; Holst, O.; Rhen, M.; Korhonen, T. K.; Lahteenmaki, K. Activation of pro-matrix metalloproteinase-9 and degradation of gelatin by the surface protease PgtE of Salmonella enterica serovar Typhimurium. *Int. J. Med. Microbiol.* **2008**, *298* (3−4), 263−78.

(32) Guina, T.; Yi, E. C.; Wang, H.; Hackett, M.; Miller, S. I. A PhoP-regulated outer membrane protease of Salmonella enterica serovar typhimurium promotes resistance to alpha-helical antimicrobial peptides. *J. Bacteriol.* **2000**, *182* (14), 4077−86.

(33) Anfinsen, C. B. Principles that govern the folding of protein chains. *Science* **1973**, *181* (4096), 223−30.

(34) Kramer, R. A.; Brandenburg, K.; Vandeputte-Rutten, L.; Werkhoven, M.; Gros, P.; Dekker, N.; Egmond, M. R. Lipopolysaccharide regions involved in the activation of Escherichia coli outer membrane protease OmpT. *Eur. J. Biochem.* **2002**, *269* (6), 1746−52.

(35) Kukkonen, M.; Korhonen, T. K. The omptin family of enterobacterial surface proteases/adhesins: from housekeeping in Escherichia coli to systemic spread of Yersinia pestis. *Int. J. Med. Microbiol.* **2004**, *294* (1), 7−14.

(36) Wu, C.; Tran, J. C.; Zamdborg, L.; Durbin, K. R.; Li, M.; Ahlf, D. R.; Early, B. P.; Thomas, P. M.; Sweedler, J. V.; Kelleher, N. L. A protease for 'middle-down' proteomics. *Nat. Methods* **2012**, *9* (8), 822−4.

(37) Sinsinbar, G.; Gudlur, S.; Metcalf, K. J.; Mrksich, M.; Nallani, M.; Liedberg, B. Role of Lipopolysaccharide in Protecting OmpT from Autoproteolysis during In Vitro Refolding. *Biomolecules* **2020**, *10* (6), 922.

(38) Kramer, R. A.; Zandwijken, D.; Egmond, M. R.; Dekker, N. In vitro folding, purification and characterization of Escherichia coli outer membrane protease ompT. *Eur. J. Biochem.* **2000**, *267* (3), 885−93.

https://doi.org/10.1021/acsbiomedchemau.1c00027
ACS Bio Med Chem Au 2022, 2, 73−83

(39) Frieden, C. Slow transitions and hysteretic behavior in enzymes. *Annu. Rev. Biochem.* **1979**, *48*, 471−89.
(40) Neet, K. E.; Ainslie, G. R., Jr. Hysteretic enzymes. *Methods Enzymol.* **1980**, *64*, 192−226.
(41) Ricard, J.; Meunier, J. C.; Buc, J. Regulatory behavior of monomeric enzymes. 1. The mnemonical enzyme concept. *Eur. J. Biochem.* **1974**, *49* (1), 195−208.
(42) Huysmans, G. H.; Baldwin, S. A.; Brockwell, D. J.; Radford, S. E. The transition state for folding of an outer membrane protein. *Proc. Natl. Acad. Sci. U. S. A.* **2010**, *107* (9), 4099−104.
(43) Moon, C. P.; Kwon, S.; Fleming, K. G. Overcoming hysteresis to attain reversible equilibrium folding for outer membrane phospholipase A in phospholipid bilayers. *J. Mol. Biol.* **2011**, *413* (2), 484−94.
(44) Wood, S. E.; Sinsinbar, G.; Gudlur, S.; Nallani, M.; Huang, C. F.; Liedberg, B.; Mrksich, M. A Bottom-Up Proteomic Approach to Identify Substrate Specificity of Outer-Membrane Protease OmpT. *Angew. Chem., Int. Ed.* **2017**, *56* (52), 16531−16535.
(45) Porter, C. M.; Miller, B. G. Cooperativity in monomeric enzymes with single ligand-binding sites. *Bioorg. Chem.* **2012**, *43*, 44−50.
(46) Lu, H. P.; Xun, L.; Xie, X. S. Single-molecule enzymatic dynamics. *Science* **1998**, *282* (5395), 1877−82.
(47) Jiang, Y.; Li, X.; Morrow, B. R.; Pothukuchy, A.; Gollihar, J.; Novak, R.; Reilly, C. B.; Ellington, A. D.; Walt, D. R. Single-Molecule Mechanistic Study of Enzyme Hysteresis. *ACS Cent. Sci.* **2019**, *5* (10), 1691−1698.
(48) Xie, Y.; Maxson, T.; Tor, Y. Fluorescent ribonucleoside as a FRET acceptor for tryptophan in native proteins. *J. Am. Chem. Soc.* **2010**, *132* (34), 11896−7.
(49) Ghisaidoobe, A. B.; Chung, S. J. Intrinsic tryptophan fluorescence in the detection and analysis of proteins: a focus on Forster resonance energy transfer techniques. *Int. J. Mol. Sci.* **2014**, *15* (12), 22518−38.
(50) Zheng, H.; Lee, S.; Llaguno, M. C.; Jiang, Q. X. bSUM: A bead-supported unilamellar membrane system facilitating unidirectional insertion of membrane proteins into giant vesicles. *J. Gen. Physiol.* **2016**, *147* (1), 77−93.
(51) Karlsson, O. Method of preparing supported lipid film membranes and use thereof. US 2002O182717A1, 2002.
(52) Viard, M.; Gallay, J.; Vincent, M.; Paternostre, M. Origin of laurdan sensitivity to the vesicle-to-micelle transition of phospholipid-octylglucoside system: a time-resolved fluorescence study. *Biophys. J.* **2001**, *80* (1), 347−59.
(53) Pinto, S. N.; Fernandes, F.; Fedorov, A.; Futerman, A. H.; Silva, L. C.; Prieto, M. A combined fluorescence spectroscopy, confocal and 2-photon microscopy approach to re-evaluate the properties of sphingolipid domains. *Biochim. Biophys. Acta, Biomembr.* **2013**, *1828* (9), 2099−110.
(54) Hritonenko, V.; Stathopoulos, C. Omptin proteins: an expanding family of outer membrane proteases in Gram-negative Enterobacteriaceae. *Mol. Membr. Biol.* **2007**, *24* (5−6), 395−406.
(55) Fernandez, C.; Hilty, C.; Wider, G.; Wuthrich, K. Lipid-protein interactions in DHPC micelles containing the integral membrane protein OmpX investigated by NMR spectroscopy. *Proc. Natl. Acad. Sci. U. S. A.* **2002**, *99* (21), 13533−7.
(56) Bond, P. J.; Sansom, M. S. Membrane protein dynamics versus environment: simulations of OmpA in a micelle and in a bilayer. *J. Mol. Biol.* **2003**, *329* (5), 1035−53.
(57) Adams, P. G.; Lamoureux, L.; Swingle, K. L.; Mukundan, H.; Montano, G. A. Lipopolysaccharide-induced dynamic lipid membrane reorganization: tubules, perforations, and stacks. *Biophys. J.* **2014**, *106* (11), 2395−407.
(58) Popot, J. L.; Engelman, D. M. Membranes Do Not Tell Proteins How To Fold. *Biochemistry* **2016**, *55* (1), 5−18.
(59) Schindelin, J.; Arganda-Carreras, I.; Frise, E.; Kaynig, V.; Longair, M.; Pietzsch, T.; Preibisch, S.; Rueden, C.; Saalfeld, S.; Schmid, B.; Tinevez, J. Y.; White, D. J.; Hartenstein, V.; Eliceiri, K.; Tomancak, P.; Cardona, A. Fiji: an open-source platform for biological-image analysis. *Nat. Methods* **2012**, *9* (7), 676−82.

https://doi.org/10.1021/acsbiomedchemau.1c00027
ACS Bio Med Chem Au 2022, 2, 73−83